Sun et al. EURASIP Journal on Wireless Communications and Networking (2016) 2016:109
DOI 10.1186/s13638-016-0597-1

EURASIP Journal on Wireless Communications and Networking

RESEARCH Open Access

Novel self-interference suppression schemes based on Dempster-Shafer theory with network coding in two-way full-duplex MIMO relay

Yanhua Sun[1,2*], Yi Yang[2], Pengbo Si[1,2], Ruizhe Yang[1,2] and Yanhua Zhang[1,2]

Abstract

A two-way full-duplex multiple-input multiple-output (MIMO) relay provides effective spectral efficiency and system capacity improvement. However, self-interference (SI) as a serious problem limits the development of a full-duplex relay. In this paper, the novel SI suppression schemes based on the Dempster-Shafer (DS) evidence theory are proposed to suppress SI in the two-way full-duplex MIMO relay. DS evidence theory can appropriately characterize uncertainty and make full use of multiple evidence source information by DS combination rule to obtain reliable decisions. The first proposed DS network coding (DS-NC) scheme adopts DS evidence theory to detect the signal of each source node, considering SI suppression in the basic probability assignment computation in the multiple access phase. Moreover, different from the DS-NC scheme, the further proposed DS physical-layer network coding (DS-PNC) scheme considers SI suppression from the vector space perspective and combines the PNC mapping rule with the DS theory to obtain a network-coded signal without estimating each source node signal. In the broadcast phase, antenna selection is adopted at the relay and DS evidence theory is also applied at each source node for SI suppression. Meanwhile, the effects of imperfect SI channel estimation and the intended channel estimation on the proposed schemes are also studied. Finally, the proposed DS-PNC scheme is studied with the SI signal model which considers analog radio frequency cancellation, the effects of I/Q modulator imbalances, and power amplifier nonlinearity of the transmitter. Simulation results reveal that the proposed DS-PNC scheme is a little more sensitive to the channel estimation errors than the traditional spatial-domain schemes. However, with the perfect channel state information, the proposed DS-NC with one iteration and DS-PNC schemes outperform traditional spatial-domain schemes. Furthermore, considering the SI signal model with nonlinear distortion and radio frequency cancellation, the DS-PNC scheme is also superior to the traditional schemes. Meanwhile, the DS-PNC scheme is more robust to the SI and achieves the same diversity gain as the ideal cancellation.

Keywords: Two-way full-duplex MIMO relay, Self-interference, Dempster-Shafer evidence theory

1 Introduction

Relaying is regarded as a key technique in cooperation communication to provide more extensive coverage and mitigate the transmit power [1]. Furthermore, the multiple-input multiple-output (MIMO) technique has attracted the most research interest and is widely used in wireless communication systems. Hence, the MIMO relay is considered as a promising technique to obtain better reliability and higher capacity. Considering the traditional two-way half-duplex (HD) MIMO relay [2–4], four orthogonal transmission phases are required to finish information exchange between two source nodes via relay. To improve the spectral efficiency, the two-way HD MIMO relay with network coding (NC) [5–7] is proposed to reduce the phases of exchanging information. Two source nodes send their own signals to the relay at the same time in the multiple access (MA) phase, and the relay

*Correspondence: sunyanhua@bjut.edu.cn
[1] Beijing Advanced Innovation Center for Future Internet Technology, Beijing University of Technology, 100124 Beijing, People's Republic of China
[2] College of Electronic Information and Control Engineering, Beijing University of Technology, 100124 Beijing, People's Republic of China

transmits the network-coded signal to each source node simultaneously in the broadcast (BC) phase. Finally, each source node detects the network-coded signal and obtains the other's transmitted signal by XOR operation. Furthermore, the physical-layer network coding (PNC) proposed in [8, 9] can obtain network-coded signal directly at the relay without estimating the signal of each source node. Recently, full-duplex (FD) communication is proposed as a potential technique to further improve the spectral efficiency, which can transmit and receive simultaneously at the same frequency band. However, the main challenge in a two-way FD MIMO relay system [10, 11] is the self-interference (SI) caused by the self-feedback signal from the relay transmitter to the receiver. At the relay input, the SI is much larger than the interested signals, which reduces the reliability and system throughput [12]. Therefore, the SI suppression in the FD relay system is considered as an important technique to enable simultaneous transmission and reception.

Various SI suppression schemes in a one-way FD relay have been proposed in earlier works. The SI suppression techniques are usually classified into passive and active suppressions. Passive SI suppression is defined as the signal power attenuation imposed by the physical separation between the transmit and receive antennas [13, 14]. Active suppression techniques are divided into analog suppression, digital suppression, and combined suppression. This paper focuses on digital baseband suppression techniques, which are subdivided into time-domain cancellation [15, 16] and spatial-domain suppression [17–25]. Time-domain cancellation cancels the SI by subtracting its own transmitted signal at the reception. However, as the MIMO technique is widely used at the relay, the biggest disadvantage of time-domain cancellation is that it cannot take full advantage of spatial-domain resources. Hence, spatial-domain suppression schemes are proposed to design different transceiver matrices to meet different system objectives, e.g., null-spacing projection [17–19], minimum mean square error (MMSE) filter [17, 18], antenna selection [20–22], maximum signal-to-interference ratio (SIR) [23], eigenbeamforming [24], and linear transceiver [25]. For a two-way FD relay, most previous researches mainly aim at improving the achievable sum rate, outage probability, capacity, and throughput with SI existing and do not consider the SI suppression problem. For example, the author in [26] compares the performances of the two-way FD and HD relays and illustrates the benefit of power optimization. The Alamouti-based scheme used in [27] enhances the capacity and outage probability without considering the SI suppression. The power allocation scheme used in [28] focuses on maximizing the sum rate of the two-way FD amplify-forward (AF) relay. Moreover, in [29], the paper mainly aims at maximizing the end-to-end sum rate by exploiting joint beamforming optimization and power control.

Recently, the Dempster-Shafer (DS) evidence theory has been proved to obtain good performance in many fields such as data fusion [30], artificial intelligence research [31], and cooperative communication [32]. In this paper, two novel SI suppression schemes based on the DS theory are proposed for the two-way FD MIMO relay system. According to the DS theory, uncertainty of the received signals caused by channel fading, SI, and noise can be characterized by the basic probability assignment (BPA) function, which is a likelihood measure and computed by the proposed probability density function (PDF) with the SI suppression considered. The first proposed scheme called DS-NC exploits the Dempster's rule to combine the BPAs from different receive antennas to explicitly estimate the signal of each source node in the MA phase. Then, the network-coded signal is achieved by XOR operation. Different from DS-NC, another SI suppression scheme called DS-PNC is proposed, which considers the SI suppression from the vector space perspective and combines the PNC mapping rule with the DS theory to directly decide the network-coded signal without estimating each source node signal. For comparison, the DS-PNC scheme is used to further suppress the SI after traditional spatial-domain schemes. In the BC phase, antenna selection [33] is adopted at the relay and DS evidence theory is also applied at each source node for SI suppression. Meanwhile, the effects of imperfect SI channel estimation and the intended channel estimation on the proposed schemes are also studied. Finally, we build a SI signal model which considers analog radio frequency (RF) cancellation, the effects of I/Q modulator imbalances, and power amplifier (PA) nonlinear distortion at the transmitter.

The rest of paper is organized as follows. Section 2 depicts a theoretical system model without nonlinear distortion considered for the two-way FD MIMO relay. In Section 3, the DS evidence theory is briefly reviewed and two SI suppression schemes based on the DS evidence theory are proposed. In Section 4, the transmit scheme adopted in the BC phase is briefly introduced. Section 5 shows the influence of channel estimation errors on the proposed schemes. In Section 6, the proposed DS-PNC scheme is studied with transmitter impairments considered. The simulation results are presented and described in Section 7. Section 8 shows the complexity analysis of the proposed schemes. Finally, Section 9 concludes the paper.

2 System model without nonlinear distortion

A two-way FD MIMO relay system is considered as Fig. 1, which consists of two source nodes and a relay node. Each source node has one transmit and two receive antennas, and the relay node has n_R receive antennas and n_T

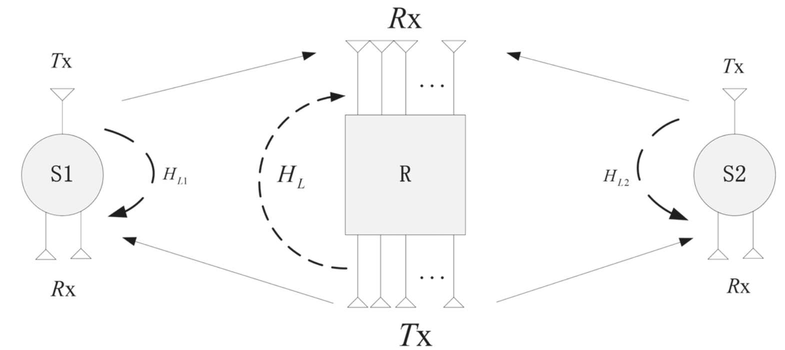

Fig. 1 Two-way FD MIMO relay system

transmit antennas. In this paper, we assume that $n_T \leq n_R$ and no direct link exists between the source nodes. Both the relay node and two source nodes work in FD mode, and physical isolation between transmit and receive antennas is considered. At the t-th time slot, each source node detects the signal of $(t-1)$-th time with a fixed delay of a single time slot. The MA, BC, and self-feedback channels are assumed to be quasi-static flat fading and remain static during the one-frame transmission phase.

In this paper, regular italics symbols, boldface lower-case symbols, boldface upper-case symbols, and regular upper-case symbols denote scalars, vectors, matrices, and sets, respectively. In the MA phase, the received signal vector in the t-th time slot at the relay is depicted as follows

$$\mathbf{y}(t) = \mathbf{H}_{MA}\mathbf{x}(t) + \mathbf{H}_L\mathbf{x}_L(t) + \mathbf{n}_R(t) \quad (1)$$

where $\mathbf{H}_{MA}$ and $\mathbf{H}_L$ denote a $n_R \times 2$ MA channel and $n_R \times n_T$ self-feedback channel, respectively. The source nodes transmit a 2×1 signal vector $\mathbf{x}(t)$, and the relay node transmits a $n_T \times 1$ signal vector $\mathbf{x}_L(t)$ while it simultaneously receives a $n_R \times 1$ signal vector $\mathbf{y}(t)$; $\mathbf{n}_R(t)$ is a $n_R \times 1$ additive white Gaussian noise vector with zero mean and variance σ^2.

The Eq. (1) can be rewritten as

$$y_i(t) = h_{ij}^{\mathrm{MA}}x_j(t) + \sum_{\substack{l=1\\ l\neq j}}^{2} h_{il}^{\mathrm{MA}}x_l(t) + \sum_{k=1}^{n_T} h_{ik}^{L}x_k^{L}(t) + n_i^{R}(t) \quad (2)$$

$$i = 1, 2, \cdots, n_R, j = 1, 2$$

where $y_i(t)$ denotes the received signal of the i-th antenna at the relay in the t-th time slot.

In the BC phase, the received signal vector at each source node can be indicated as

$$\mathbf{r}_{si}(t) = \mathbf{H}_i^{BC}\mathbf{x}_L(t) + \mathbf{H}_{Li}x_i(t) + \mathbf{n}_{si}(t) \quad i = 1, 2 \quad (3)$$

where $\mathbf{r}_{si}(t)$ denotes the received signal vector at the i-th source node, $\mathbf{H}_i^{BC}$ is the corresponding $2 \times n_T$ BC channel submatrix for each source node, $\mathbf{H}_{Li}$ denotes the 2×1 self feedback channel of the i-th source node, and $\mathbf{n}_{si}(t)$ is the white Gaussian noise vector.

3 The proposed self-interference suppression schemes based on Dempster-Shafer evidence theory

In this section, the basic concept of the DS evidence theory [34] is briefly reviewed at first, then two novel SI suppression schemes based on the DS evidence theory are proposed to obtain better bit error rate (BER) performance.

3.1 A brief review of Dempster-Shafer evidence theory

The DS evidence theory is a generalization of the Bayes theory, which is based on the constructive interpretation of probability proposed by Shafer. The constructive interpretation of probability emphasizes not only the importance of objective evidence but also the importance of subjective estimation. So, it can fully characterize the uncertainty of propositions. Let Θ indicate the finite set which contains mutually exclusive and exhaustive hypotheses, called the framework of discernment. All subsets of the framework of discernment constitute a power set 2^{Θ}. After establishing the concept of framework of discernment, Shafer presents a mathematical model for evidence processing as shown in Fig. 2.

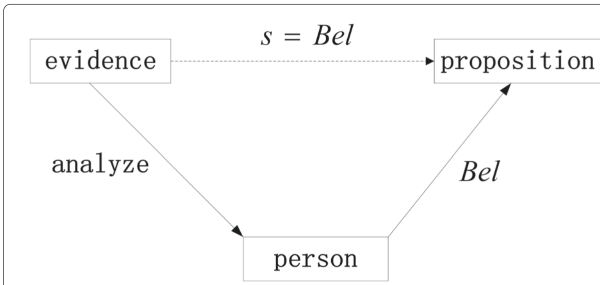

Fig. 2 Mathematical model for evidence processing

The knowledge about the hypothetical propositions produces a BPA function, which is defined as a function $m(\cdot)$ from the power set 2^{Θ} mapping to the interval $[0, 1]$ as follows

$$m(\Phi) = 0 \quad (4)$$

$$\forall A \subset \Theta, m(A) \geq 0 \quad (5)$$

$$\sum_{\forall A \subseteq \Theta} m(A) = 1 \quad (6)$$

where Φ is a null set and each subset $A \subset \Theta$ is called a focal element set (FES), which satisfies $m(A) \geq 0$. Based on the BPA function $m(A)$, belief function $\mathrm{Bel}(A)$ can be expressed as

$$\mathrm{Bel}(A) = \sum_{B \subseteq A} m(B) \quad (7)$$

The belief function $\mathrm{Bel}(A)$ denotes the total belief assigned to the proposition A. It is important for the DS evidence theory to combine several different evidences from the same framework of discernment through Dempster's combining rule, which is defined as the orthogonal sum [34, 35]. We assume that $\mathrm{Bel}_1, \ldots, \mathrm{Bel}_n$ are belief functions of the same framework of discernment and $m_1, \ldots, m_n$ are the corresponding BPAs. If $\mathrm{Bel}_1 \oplus \cdots \oplus \mathrm{Bel}_n$ exists, Dempster's combining rule can be expressed as follows [36]

$$\begin{aligned} &\forall A \subset \Theta, A \neq \Phi \\ &m(A) = k \cdot \sum_{\substack{A^1 \cdots A^n \subset \Theta \\ A^1 \cap \cdots \cap A^n = A}} m_1(A^1) \cdots m_n(A^n) \end{aligned} \quad (8)$$

where the normalization coefficient k is shown as

$$k = \left(\sum_{\substack{A^1 \cdots A^n \subset \Theta \\ A^1 \cap \cdots \cap A^n \neq \Phi}} m_1(A^1) \cdots m_n(A^n) \right)^{-1} \quad (9)$$

where A^n denotes the FES for the n-th evidence source. The normalization coefficient k denotes the conflict among several different evidences. DS theory can combine multiple evidences to counteract uncertainty contained in different evidences and make a more reliable decision.

In this paper, the frame of discernment is selected as modulation constellation set Ψ. A FES $A \subset \Psi$ contains some constellation points. For example, $A = \{\varphi_a\}$ or $A = \{\varphi_a, \varphi_b\}$ or $A = \{\varphi_a, \varphi_b, \varphi_c\} \cdots$, where $\varphi_a, \varphi_b, \varphi_c$ are constellation points and $a \neq b \neq c, a, b, c = 1, 2, \cdots, M$. M is the modulation constellation set cardinality. FES A represents the uncertainty of decisions. For example, $A = \{\varphi_a, \varphi_b\}$ implies that the transmitted signal is likely to be φ_a or φ_b. That is, the more elements FES A contains, the more uncertainty it reflects. DS theory characterizes this uncertainty of FES A by BPA function $m(A)$. Actually, the $m(A)$ can be defined by several methods such as the cumulative density function (CDF) and probability density function (PDF). In this paper, PDF is used to denote the BPA of a FES A. From the above description, we can see that the complexity of the algorithm increases with the number of FES. In this paper, Binary Phase Shift Keying (BPSK) and Quadrature Phase Shift Keying (QPSK) modulation are considered. For BPSK modulation, all the FESs such as single-point set $A_1 = \{-1\}, A_1 = \{1\}$ and two-point set $A_2 = \{-1, 1\}$ are considered because the number of FES is only three. For high order modulation, due to large number of FES, the FES which only contains single-point or two-point is considered for simplicity. The following sections will discuss the proposed SI suppression schemes based on the DS theory in details.

3.2 The proposed Dempster-Shafer network coding scheme for self-interference suppression in two-way full-duplex MIMO relay

Different from traditional spatial-domain suppression schemes, the DS-NC scheme employs the DS evidence theory to estimate the signal of each source node and suppresses the SI without designing the transceiver filter matrices.

In DS-NC, the decision statistics of each source node needs to be obtained at each receive antenna for BPA computation. However, due to SI, the decreased accuracy of decision statistics leads to the bad performance of DS-NC. Hence, the iteration method is adopted for BPA computation to mitigate this problem.

First, for each transmitted signal from each source node, there are n_R decision statistics at the relay. According to Eq. (2), the n_R decision statistics of the j-th source node signal x_j is shown as

$$\hat{x}_{ij}(t) = h_{ij}^{MA^{-1}} \left[y_i(t) - \sum_{\substack{l=1 \\ l \neq j}}^{2} h_{il}^{MA} \tilde{x}_l(t) \right], i = 1, \cdots, n_R, j = 1, 2 \quad (10)$$

where $\tilde{x}_l(t)$ denotes the initial estimation as follows

$$\tilde{x}_l(t) = \mathbf{w}_l \mathbf{y}(t) = x_l(t) + \mathbf{w}_l \mathbf{H}_L \mathbf{x}_L(t) + \mathbf{w}_l \mathbf{n}_R(t), l = 1, 2 \quad (11)$$

where $\mathbf{w}_l$ denotes a zero-forcing (ZF) linear detection weight vector for the l-th source. Substitute Eqs. (2) and (11) into Eq. (10), then Eq. (10) is rewritten as

$$\begin{aligned}
\hat{x}_{ij}(t) &= h_{ij}^{\mathrm{MA}^{-1}} \left[h_{ij}^{\mathrm{MA}} x_j(t) + \sum_{\substack{l=1\\ l\neq j}}^{2} h_{il}^{\mathrm{MA}} x_l(t) + \sum_{k=1}^{n_T} h_{ik}^{L} x_k^{L}(t) + n_i^{R}(t) \right. \\
&\quad \left. - \sum_{\substack{l=1\\ l\neq j}}^{2} h_{il}^{\mathrm{MA}} (x_l(t) + \mathbf{w}_l \mathbf{H}_L \mathbf{x}_L(t) + \mathbf{w}_l \mathbf{n}_R(t)) \right] \\
&= x_j(t) - h_{ij}^{\mathrm{MA}^{-1}} \left[- \sum_{k=1}^{n_T} h_{ik}^{L} x_k^{L}(t) + \sum_{\substack{l=1\\ l\neq j}}^{2} h_{il}^{\mathrm{MA}} \mathbf{w}_l \mathbf{H}_L \mathbf{x}_L(t) \right. \\
&\quad \left. + \sum_{\substack{l=1\\ l\neq j}}^{2} h_{il}^{\mathrm{MA}} \mathbf{w}_l \mathbf{n}_R(t) - n_i^{R}(t) \right] \\
&= x_j(t) - h_{ij}^{\mathrm{MA}^{-1}} \left[-\mathbf{h}_i^{L} \mathbf{x}_L(t) + \sum_{\substack{l=1\\ l\neq j}}^{2} h_{il}^{\mathrm{MA}} \mathbf{w}_l \mathbf{H}_L \mathbf{x}_L(t) \right. \\
&\quad \left. + \sum_{\substack{l=1\\ l\neq j}}^{2} h_{il}^{\mathrm{MA}} (w_{l1} n_1^{R}(t) + \cdots + w_{li} n_i^{R}(t) + \cdots + w_{ln_R} n_{in_R}^{R}(t)) - n_i^{R}(t) \right] \\
&= x_j(t) - h_{ij}^{\mathrm{MA}^{-1}} \left[\left(-\mathbf{h}_i^{L} + \sum_{\substack{l=1\\ l\neq j}}^{2} h_{il}^{\mathrm{MA}} \mathbf{w}_l \mathbf{H}_L \right) \mathbf{x}_L(t) + \breve{n}_i^{R}(t) \right]
\end{aligned} \tag{12}$$

where the $\mathbf{h}_i^L$ denotes the i-th row of self-feedback channel matrix $\mathbf{H}_L$ and the equivalent noise $\breve{n}_i^R(t)$ can be expressed as

$$\begin{aligned}
\breve{n}_i^{R}(t) &= \breve{\mathbf{g}}_i \mathbf{n}_R(t) \\
\breve{\mathbf{g}}_i &= \left[\sum_{\substack{l=1\\ l\neq j}}^{2} h_{il}^{\mathrm{MA}} w_{l1}, \cdots, \sum_{\substack{l=1\\ l\neq j}}^{2} h_{il}^{\mathrm{MA}} w_{li} - 1, \cdots, \sum_{\substack{l=1\\ l\neq j}}^{2} h_{il}^{\mathrm{MA}} w_{ln_R} \right]
\end{aligned} \tag{13}$$

In this paper, the BPA $m_{ij}(A)$ of each FES A is defined as the conditional PDF of decision statistics $\hat{x}_{ij}(t)$. According to Eq. (12), $\hat{x}_{ij}(t)$ is a complex Gaussian random variable with mean $x_j(t) - h_{ij}^{\mathrm{MA}^{-1}}(-\mathbf{h}_i^L + \sum_{l=1,l\neq j}^{2} h_{il}^{\mathrm{MA}} \mathbf{w}_l \mathbf{H}_L)\mathbf{x}_L(t)$ and variance $\parallel h_{ij}^{\mathrm{MA}^{-1}} \breve{\mathbf{g}}_i \parallel^2 \sigma^2$. The vector $\mathbf{x}_L(t)$ belongs to the set Ω which contains M^{n_T} possible vectors (for BPSK modulation, $M = 2$; for QPSK modulation, $M = 4$). So, the conditional PDF of $\hat{x}_{ij}(t)$ can be written as

$$\begin{aligned}
& f(\hat{x}_{ij}(t) \mid \alpha(A)) \quad \forall A \subset U \\
&= \sum_{\mathbf{x}_L(t)\in\Omega} \frac{1}{\sqrt{2\pi \parallel h_{ij}^{\mathrm{MA}^{-1}} \breve{\mathbf{g}}_i \parallel^2 \sigma^2}} \exp\left[\frac{-\parallel \hat{x}_{ij}(t) - \alpha(A) + L \parallel^2}{2 \parallel h_{ij}^{\mathrm{MA}^{-1}} \breve{\mathbf{g}}_i \parallel^2 \sigma^2} \right] \\
L &= h_{ij}^{\mathrm{MA}^{-1}} \left(-\mathbf{h}_i^{L} + \sum_{\substack{l=1\\ l\neq j}}^{2} h_{il}^{\mathrm{MA}} \mathbf{w}_l \mathbf{H}_L \right) \mathbf{x}_L(t)
\end{aligned} \tag{14}$$

where U is the set that contains all the considered FESs and $\alpha(A)$ denotes the eigenvalue of FES A, which is defined as the mean of all elements of FES A [34, 35]. As shown in Eq. (14), the SI is considered as a part of the expectation of $\hat{x}_{ij}(t)$ in the BPA computation. According to the DS theory, BPA $m_{ij}(A)$ must be normalized to satisfy Eq. (6) and is written as

$$m_{ij}(A) = r_{ij} \cdot f(\hat{x}_{ij}(t) \mid \alpha(A)), \forall A \subset U \tag{15}$$

where r_{ij} is the normalization coefficient expressed as

$$r_{ij} = \frac{1}{\sum_{\forall A\subset U} f(\hat{x}_{ij}(t) \mid \alpha(A))} \tag{16}$$

Then Dempster's combination rule Eq. (8) is applied to combine the BPAs $m_{ij}(A)$ from each receive antenna and the $m_j(A)$ for each source node is obtained. In [34] and [35], a least point decision (LPD) rule is proposed to make a final decision as follows

$$\begin{aligned}
\bar{A}_{n-1} &= \underset{A_{n-1}\subset U}{\operatorname{argmax}} \mathrm{BPA}(A_{n-1}) \\
\bar{A}_{n-2} &= \underset{A_{n-2}\subset \bar{A}_{n-1}}{\operatorname{argmax}} \mathrm{BPA}(A_{n-2}) \\
&\vdots \\
\bar{A}_{1} &= \underset{A_{1}\subset \bar{A}_{2}}{\operatorname{argmax}} \mathrm{BPA}(A_{1})
\end{aligned} \tag{17}$$

where A_n denotes the FES that has n constellation points. $\bar{A}_{n-1}$ is the FES which has the maximum credibility in all the FESs which satisfy $A_{n-1} \subset U$. For LPD, $n-1$ comparisons are needed. In order to reduce the decision complexity, a maximum single-point credibility (MC) rule is adopted to decide the signal estimation $\hat{x}_j(t)$ corresponding to the maximum $\mathrm{BPA}(A_1)$ as follows

$$\bar{A}_1 = \max \mathrm{BPA}(A_1) \tag{18}$$

where $\bar{A}_1$ is the FES which has the maximum credibility among all the single-point FESs.

Although the signal estimation $\hat{x}_j(t)$ is obtained at the relay, the result is not good because of inaccurate initial estimation. In order to further enhance the estimation performance, $\hat{x}_j(t)$ instead of the initial estimation $\tilde{x}_l(t)$ is substituted into Eq. (10), then the BPA $m_j(A_1)$ is computed again by Eqs. (8), (14), and (15). The final signal estimation is decided according to the MC rule. In this paper, we only use one iteration in DS-NC for complexity problem. Finally, the network-coded signal $x_1 \oplus x_2$ is obtained by XOR operation at the relay (for QPSK modulation, the XOR operation is applied for the in-phase part and the quadrature-phase part).

3.3 The proposed Dempster-Shafer physical-layer network coding scheme for self-interference suppression in two-way full-duplex MIMO relay

3.3.1 The proposed Dempster-Shafer physical-layer network coding scheme

DS-NC is suboptimal because it still comes from the virtual MIMO perspective. However, the DS-PNC scheme is proposed from the vector space perspective, which combines the PNC mapping rule and DS evidence theory to directly obtain the network-coded signal with the SI considered in the BPA computation. In the DS-PNC scheme, the modulation constellation set is also selected as the framework of discernment. For BPSK modulation, three FESs are considered, e.g., $A_1 = \{-1\}$ or $A_1 = \{1\}$ or $A_2 = \{-1, 1\}$. According to the PNC mapping rule, the combined transmit vector $\mathbf{x}_s(t) = [x_1(t), x_2(t), \mathbf{x}_L(t)]^T$ is divided into two groups corresponding to $x_1 \oplus x_2 = 1$ and $x_1 \oplus x_2 = -1$. The number of elements in each group is decided by the number of transmit antennas n_T at the relay, and each group contains 2^{n_T+1} candidate vectors. One group $B = \{[-1, 1, \mathbf{x}_L(t)]^T, [1, -1, \mathbf{x}_L(t)]^T\}$ corresponds to $x_1 \oplus x_2 = 1$, and the other group $C = \{[-1, -1, \mathbf{x}_L(t)]^T, [1, 1, \mathbf{x}_L(t)]^T\}$ corresponds to $x_1 \oplus x_2 = -1$. The vector $\mathbf{x}_L(t)$ also belongs to the set Ω presented in DS-NC. Different from DS-NC, the BPA $m(A)$ is defined as a conditional PDF of the received signal $y_i(t)$. For all single-point FESs A_1, the conditional PDF of $y_i(t)$ can be written as

$$
\begin{aligned}
& f(y_i(t) \mid x_1 \oplus x_2 = -1) \\
& = \frac{1}{\sqrt{2\pi\sigma^2}} \sum_{\mathbf{x}_s(t) \in C} \exp\left[\frac{\| y_i(t) - (h_{i1}^{\mathrm{MA}}, h_{i2}^{\mathrm{MA}}, \mathbf{h}_i^L)\mathbf{x}_s(t) \|^2}{2\sigma^2}\right] \\
& f(y_i(t) \mid x_1 \oplus x_2 = 1) \\
& = \frac{1}{\sqrt{2\pi\sigma^2}} \sum_{\mathbf{x}_s(t) \in B} \exp\left[\frac{\| y_i(t) - \left(h_{i1}^{\mathrm{MA}}, h_{i2}^{\mathrm{MA}}, \mathbf{h}_i^L\right) \mathbf{x}_s(t) \|^2}{2\sigma^2}\right] \\
& i = 1, \cdots, n_R
\end{aligned} \tag{19}
$$

where σ^2 denotes the variance of additional Gaussian white noise $\mathbf{n}_R(t)$ and $\mathbf{h}_i^L$ is the i-th row of the self-feedback channel matrix.

For two-point FES A_2, the conditional PDF is defined as the sum of the PDFs for all single-point FESs A_1 as follows

$$f(y_i \mid \alpha(A_2)) = f(y_i \mid x_1 \oplus x_2 = -1) + f(y_i \mid x_1 \oplus x_2 = 1) \tag{20}$$

where $\alpha(A_2)$ denotes the eigenvalue of FES A_2 defined as the mean of vectors for each FES.

For the QPSK modulation, four single-point FESs and six two-point FESs are considered for BPA computation. According to the PNC mapping rule for the in-phase and quadrature-phase parts of a QPSK symbol, vector $\mathbf{x}_s(t)$ is divided into four groups denoted by λ_k, $k = 1, 2, \cdots, 4$. Each group contains 4^{n_T+1} vectors which are decided by the number of transmit antennas n_T at the relay. For example, the group $\lambda_1 = \{[-1-j, 1+j, \mathbf{x}_L(t)]^T, [-1+j, 1-j, \mathbf{x}_L(t)]^T, [1-j, -1+j, \mathbf{x}_L(t)]^T, [1+j, -1-j, \mathbf{x}_L(t)]^T\}$ corresponds to $x_1 \oplus x_2 = (1+j)$. The other groups λ_2, λ_3, and λ_4 correspond to $x_1 \oplus x_2 = (-1+j)$, $x_1 \oplus x_2 = (1-j)$, $x_1 \oplus x_2 = (-1-j)$, respectively. The vector $\mathbf{x}_L(t)$ also belongs to the set Ω that contains 4^{n_T} candidate vectors. For the single-point FES in QPSK, similar to the case of BPSK, the conditional PDF is described as

$$
\begin{aligned}
f(y_i(t) \mid \alpha(A_1)) = & \frac{1}{\sqrt{2\pi\sigma^2}} \sum_{\mathbf{x}_s(t) \in \lambda_k} \\
& \exp\left[\frac{\| y_i(t) - \left(h_{i1}^{\mathrm{MA}}, h_{i2}^{\mathrm{MA}}, \mathbf{h}_i^L\right) \mathbf{x}_s(t) \|^2}{2\sigma^2}\right] \\
k = 1, 2, \cdots, 4 &
\end{aligned} \tag{21}
$$

For high order modulation, the BPA computation is different from the case of BPSK , which is based on the fact that the BPA of multi-point FES mainly depends on the minimum BPA of its own contained single-point FES [32]. So, the conditional PDF is denoted by

$$f(y_i(t) \mid \alpha(A_2)) = \min_{A_1 \subset A_2} f(y_i(t) \mid \alpha(A_1)) \tag{22}$$

Similar to DS-NC, BPA $m_i(A)$ of the i-th receive antenna must be normalized to satisfy Eq. (6) and is written as

$$m_i(A) = r_i \cdot f(y_i(t) \mid \alpha(A)), \quad \forall A \subset U \tag{23}$$

where U is the set that contains all the considered FESs and r_i is the normalization coefficient, indicated by

$$r_i = \frac{1}{\sum_{\forall A \subset U} f(y_i(t) \mid \alpha(A))} \tag{24}$$

After obtaining the BPA $m_i(A)$ of FES A, Dempster's combination rule is applied to combine the BPAs $m_i(A)$ from each receive antenna. Then, the final decision of network-coded signal $x_1 \oplus x_2$ is decided by the maximum $m(A_1)$ according to the MC rule.

3.3.2 The combination of Dempster-Shafer physical-layer network coding and minimum mean square error scheme

For comparison, the proposed DS-PNC scheme combined with the MMSE spatial-domain scheme is presented in this part. In fact, DS-PNC regarded as the detection algorithm is applied to further suppress the SI after the traditional MMSE spatial-domain scheme.

In the MMSE suppression scheme, considering transceiver filter matrices at the relay, Eq. (1) can be rewritten as follows

$$\widehat{\mathbf{y}}_{mmse}(t) = \mathbf{H}_{MA}^{eq}\mathbf{x}(t) + \mathbf{H}_L^{eq}\mathbf{x}_L(t) + \mathbf{n}_R^{eq}(t) \tag{25}$$

where $\mathbf{H}_{MA}^{eq} = \mathbf{G}_{rx}\mathbf{H}_{MA}$, $\mathbf{H}_{L}^{eq} = \mathbf{G}_{rx}\mathbf{H}_{L}\mathbf{G}_{tx}$, and $\mathbf{n}_{R}^{eq} = \mathbf{G}_{rx}\mathbf{n}_{R}$ are the equivalent MA channel, self-feedback channel, and noise vector, respectively. For BPSK modulation, substitute Eq. (25) into Eq. (19), then the BPAs of all single-point FESs can be expressed as

$$
\begin{aligned}
& f(\hat{y}_i^{\text{mmse}}(t) \mid x_1 \oplus x_2 = -1) \\
& = \frac{1}{\sqrt{2\pi\sigma_{\text{ieq}}^2}} \sum_{\mathbf{x}_s(t)\in C} \exp\left[\frac{\| \hat{y}_i^{\text{mmse}}(t) - \left(h_{i1}^{\text{MAeq}}, h_{i2}^{\text{MAeq}}, \mathbf{h}_i^{Leq}\right)\mathbf{x}_s(t) \|^2}{2\sigma_{ieq}^2}\right] \\
& f(\hat{y}_i^{\text{mmse}}(t) \mid x_1 \oplus x_2 = 1) \\
& = \frac{1}{\sqrt{2\pi\sigma_{\text{ieq}}^2}} \sum_{\mathbf{x}_s(t)\in B} \exp\left[\frac{\| \hat{y}_i^{\text{mmse}}(t) - \left(h_{i1}^{\text{MAeq}}, h_{i2}^{\text{MAeq}}, \mathbf{h}_i^{Leq}\right)\mathbf{x}_s(t) \|^2}{2\sigma_{\text{ieq}}^2}\right] \\
& i = 1, \cdots, n_R
\end{aligned}
\tag{26}
$$

where h_{i1}^{MAeq} and h_{i2}^{MAeq} denote the elements of the equivalent MA channel matrix, $\mathbf{h}_i^{Leq}$ is the i-th row vector of the equivalent self-feedback channel matrix, $\hat{y}_i^{\text{mmse}}(t)$ denotes the i-th row of the received signal $\widehat{\mathbf{y}}_{mmse}(t)$, and σ_{ieq}^2 denotes the equivalent noise variance at the i-th receive antenna that can be written as

$$
\sigma_{\text{ieq}}^2 = \left[\mathbf{g}_i^{rx}\mathbf{g}_i^{rxH}\right]\sigma^2 \tag{27}
$$

where $\mathbf{g}_i^{rx}$ denotes the i-th row vector of the MMSE receive filter matrix $\mathbf{G}_{rx}$. For QPSK, the BPA computation for single-point FES is obtained by substituting Eq. (25) into Eq. (21).

For two-point FES, the BPA computation is still defined as Eqs. (20) and (22) for the BPSK and QPSK modulations, respectively. After obtaining the BPAs of all the FESs, Dempster's combination rule and the MC rule are used to obtain the network-coded symbol.

3.4 The Dempster-Shafer scheme for self-interference suppression at the source nodes

Considering the model presented in Section 2, the SI still exists at each source node and the DS theory is again applied to suppress the SI from vector perspective. But different from the DS-NC and DS-PNC schemes, initial signal estimation and PNC mapping rule are not needed at the source nodes. The modulation constellation set Ψ still acts as the framework of discernment. The combined transmit vector $\mathbf{x}_{ri}(t) = [\mathbf{x}_L(t), x_i(t)]^T$ is divided into two groups for BPSK and four groups for QPSK. According to Eq. (3), for the j-th receive antenna of the i-th source node, the BPA computation of all single-point FES can be denoted as

$$
\begin{aligned}
& f(r_{sij}(t) \mid \alpha(A_1)) \\
& = \frac{1}{\sqrt{2\pi\sigma^2}} \sum_{x_i(t)\in\Psi} \exp\left[\frac{\| r_{sij}(t) - (\mathbf{h}_j^{BCi}, h_j^{Lsi})\mathbf{x}_{ri}(t) \|^2}{2\sigma^2}\right] \\
& i = 1, 2 \quad j = 1, 2
\end{aligned}
\tag{28}
$$

where $r_{sij}(t)$ denotes the received signal of the j-th antenna at the i-th source node, $\mathbf{h}_j^{BCi}$ denotes the BC channel vector for the j-th receive antenna of the i-th source node, and h_j^{Lsi} is the j-th row of the self-feedback channel matrix $\mathbf{H}_{Li}$ for the i-th source node. For two-point FES, the BPA computation is similar to the method in the proposed DS-PNC schemes.

4 The transmit scheme in the BC phase

After transmission in the MA phase, the network-coded signal is obtained by the proposed schemes at the relay. In order to enhance the end-to-end BER performance, the BC transmission is also expected with high reliability. In the BC phase, how to exploit the channel state information at the transmitter (CSIT) is the main concern for designing the BC phase scheme. According to [34], antenna selection (AS) can obtain better performance with lower complexity. Therefore, one relay antenna is selected to transmit the network-coded signal according to the max-min singular value method. First, for each source node, n_T singular values are obtained by singular value decomposition (SVD) of the channel from each relay transmit antenna to the source node, denoted by η_{ij} $(j = 1, 2, \cdots, n_T \quad i = 1, 2)$. For each relay transmit antenna $j \in \{1, 2, \cdots, n_T\}$, the source node corresponding to the minimum value of η_{ij} is selected as follows

$$
k(j) = \arg\min_i |\eta_{ij}|, \quad i = 1, 2 \tag{29}
$$

Second, the relay transmit antenna l is selected as follows

$$
l = \arg\max_j |\eta_{k(j)j}|, \quad j = 1, 2, \cdots, n_T \tag{30}
$$

Then the antenna l is exploited to broadcast the network-coded symbol to the two source nodes.

5 The effect of channel estimation errors on the proposed schemes in the MA phase

The accurate CSI at the source and relay nodes is important for the proposed scheme. Several channel estimation methods are studied to obtain CSI in a two-way relay system [37, 38]. In this section, the effect of channel estimation errors on the proposed schemes is studied. We assume that the true channel values for the MA and self-feedback channel are denoted by

$$
\begin{aligned}
\mathbf{H}_{MA} &= \hat{\mathbf{H}}_{MA} + \Delta\mathbf{H}_{MA} \\
\mathbf{H}_{L} &= \hat{\mathbf{H}}_{L} + \Delta\mathbf{H}_{L}
\end{aligned}
\tag{31}
$$

where $\hat{\mathbf{H}}_{MA}$ and $\hat{\mathbf{H}}_L$ denote the estimation values of the MA and self-feedback channels and $\Delta\mathbf{H}_{MA}$ and $\Delta\mathbf{H}_L$ are channel estimation error matrices, whose elements are Gaussian random variables with zero mean, variances ${\sigma^2}_{\Delta h_{\mathrm{MA}}}$ and ${\sigma^2}_{\Delta h_L}$, respectively. After considering channel estimation errors, Eq. (1) is rewritten as

$$\begin{aligned}\mathbf{y}(t) = \ & \hat{\mathbf{H}}_{MA}\mathbf{x}(t) + \hat{\mathbf{H}}_L\mathbf{x}_L(t) + \Delta\mathbf{H}_{MA}\mathbf{x}(t) \\ & + \Delta\mathbf{H}_L\mathbf{x}_L(t) + \mathbf{n}_R(t)\end{aligned} \quad (32)$$

In this paper, the channel estimation errors are regarded as a part of noise, defining the equivalent noise as $\mathbf{n}_{eq} = \Delta\mathbf{H}_{MA}\mathbf{x}(t) + \Delta\mathbf{H}_L\mathbf{x}_L(t) + \mathbf{n}_R(t)$. For the proposed DS-PNC scheme, the BPA computation of single-point FES for BPSK can be denoted by

$$\begin{aligned}& f(y_i(t) \mid x_1 \oplus x_2 = -1) \\ & = \frac{1}{\sqrt{2\pi{\sigma^2}_{\mathrm{total}}}} \sum_{\mathbf{x}_s(t)\in C} \exp\left[\frac{\| y_i(t) - (\hat{h}_{i1}^{\mathrm{MA}}, \hat{h}_{i2}^{\mathrm{MA}}, \hat{\mathbf{h}}_i^L)\mathbf{x}_s(t) \|^2}{2\sigma_{\mathrm{total}}^2}\right] \\ & f(y_i(t) \mid x_1 \oplus x_2 = 1) \\ & = \frac{1}{\sqrt{2\pi\sigma_{\mathrm{total}}^2}} \sum_{\mathbf{x}_s(t)\in B} \exp\left[\frac{\| y_i(t) - (\hat{h}_{i1}^{\mathrm{MA}}, \hat{h}_{i2}^{\mathrm{MA}}, \hat{\mathbf{h}}_i^L)\mathbf{x}_s(t) \|^2}{2\sigma_{\mathrm{total}}^2}\right] \\ & i = 1, \cdots, n_R\end{aligned} \quad (33)$$

where $\hat{h}_{i1}^{\mathrm{MA}}$ and $\hat{h}_{i2}^{\mathrm{MA}}$ denote the elements of the estimated channel matrix $\hat{\mathbf{H}}_{MA}$ and $\hat{\mathbf{h}}_i^L$ is the i-th row vector of the estimated self-feedback channel matrix $\hat{\mathbf{H}}_L$. The sets C and B are the same with the ones mentioned above. The equivalent noise variance ${\sigma^2}_{\mathrm{total}}$ at the i-th receive antenna is denoted by

$${\sigma^2}_{\mathrm{total}} = \sigma^2 + n_{st} \cdot {\sigma^2}_{\Delta h_{\mathrm{MA}}} + n_T \cdot {\sigma^2}_{\Delta h_L} \quad (34)$$

where n_{st} denotes the number of transmit antennas from all the source nodes.

For QPSK, the BPA computation for single-point FES is obtained by substituting Eq. (32) into Eq. (21). For two-point FES, the BPA computation is still defined as Eqs. (20) and (22) for the BPSK and QPSK modulations, respectively.

6 The Dempster-Shafer physical-layer network coding scheme under the self-interference signal model with nonlinear distortion

6.1 The self-interference signal model with nonlinear distortion

In this paper, we build a SI signal model which includes radio frequency (RF) analog cancellation, the effects of PA nonlinearity, and I/Q imbalance of the transmitter. For simplicity, we assume the receiver I/Q imbalance can be calibrated with some methods [39].

The digital baseband signal of relay transmitter j is denoted as $s_j(t)$, and the output signal of I/Q modulator model is written as follows [39]

$$s_j^{\mathrm{IQM}}(t) = g_{1,j}s_j(t) + g_{2,j}s_j^*(t) \quad (35)$$

with the imbalance coefficients given as

$$g_{1,j} = \frac{1 + \rho_j \exp(j\varphi_j)}{2}, g_{2,j} = \frac{1 - \rho_j \exp(j\varphi_j)}{2} \quad (36)$$

where ρ_j and φ_j denote the gains and phase imbalance parameters of transmitter j, respectively. Actually, the imbalance coefficients $g_{1,j}$ and $g_{2,j}$ are satisfied with $|g_{1,j}| \gg |g_{2,j}|$ for any practical transmitter front end.

The basic memoryless nonlinear model for PA is adopted in this paper, which can be explicitly represented by Taylor's series [40, 41]. So, the P-order PA nonlinear model with Taylor's series is denoted by

$$s_j^{\mathrm{PA}}(t) = \sum_{\substack{p=1 \\ p\ \mathrm{odd}}}^{P} a_{p,j}(s_j^{\mathrm{IQM}}(t))^p \quad (37)$$

where $a_{p,j}$ is Taylor's series coefficient and $s_j^{\mathrm{PA}}(t)$ is the output signal of PA at the relay transmitter j. Then, substituting Eq. (35) into Eq. (37), $s_j^{\mathrm{PA}}(t)$ is rewritten as

$$\begin{aligned}s_j^{\mathrm{PA}}(t) & = \sum_{\substack{p=1 \\ p\ \mathrm{odd}}}^{P} a_{p,j}(g_{1,j}s_j(t) + g_{2,j}s_j^*(t))^p \\ & = \sum_{\substack{p=1 \\ p\ \mathrm{odd}}}^{P} \sum_{q=0}^{p} a_{p,j}^{(q,p-q)} \times s_j(t)^q s_j^*(t)^{(p-q)}\end{aligned} \quad (38)$$

where $a_{p,j}^{(q,p-q)}$ denotes the coefficient for the basis function $s_j(t)^q s_j^*(t)^{(p-q)}$. The order p only considers an odd number ($p = 1, 3, 5, \cdots$) , such as for $p = 1$

$$\begin{aligned}a_{1,j}^{(0,1)} & = a_{1,j}g_{2,j} \\ a_{1,j}^{(1,0)} & = a_{1,j}g_{1,j}\end{aligned}$$

and for $p = 3$ as

$$\begin{aligned}a_{3,j}^{(0,3)} & = a_{3,j}{g_{2,j}}^3 \\ a_{3,j}^{(1,2)} & = 3a_{3,j}g_{1,j}{g_{2,j}}^2 \\ a_{3,j}^{(2,1)} & = 3a_{3,j}{g_{1,j}}^2g_{2,j} \\ a_{3,j}^{(3,0)} & = a_{3,j}{g_{1,j}}^3\end{aligned}$$

The other higher orders are computed similarly but are not written out in this part.

In this paper, the SI channel model is assumed to be quasi-static flat fading and Eq. (1) can be rewritten as

$$\mathbf{y}(t) = \mathbf{H}_{MA}\mathbf{x}(t) + \sqrt{E_s}\mathbf{H}^{SI}\mathbf{s}^{PA}(t) + \mathbf{n}_R(t) \quad (39)$$

where $\mathbf{H}^{SI}$ denotes the $n_R \times n_T$ actual SI channel matrix and the PA output signal vector is $\mathbf{s}^{PA}(t) = [s_1^{PA}(t), s_2^{PA}(t), \cdots, s_{n_T}^{PA}(t)]^T$. For simplicity, we assume the transmit power of each relay antenna is satisfied with $E\{|\sqrt{E_s}s_j^{\mathrm{PA}}(t)|^2\} = 1$, $E_s = \sum_{s_j(t)\in\Psi} |\sum_{\substack{p=1\\p\,\mathrm{odd}}}^{P} \sum_{q=0}^{p} a_{p,j}^{(q,p-q)} \times s_j(t)^q s_j^*(t)^{(p-q)}|^2$ denotes the power normalization coefficient, and Ψ is the modulation constellation point set. The received signal at the i-th relay receiver is denoted by

$$\begin{aligned} y_i(t) &= h_{ij}^{\mathrm{MA}} x_j(t) + \sum_{\substack{l=1\\l\neq j}}^{2} h_{il}^{\mathrm{MA}} x_l(t) + \sum_{k=1}^{n_T} h_{ik}^{\mathrm{SI}} \sqrt{E_s} s_k^{\mathrm{PA}}(t) + n_i^R(t) \\ &= h_{ij}^{\mathrm{MA}} x_j(t) + \sum_{\substack{l=1\\l\neq j}}^{2} h_{il}^{\mathrm{MA}} x_l(t) \\ &\quad + \sum_{k=1}^{n_T} \sum_{\substack{p=1\\p\,\mathrm{odd}}}^{P} \sum_{q=0}^{p} h_{ik}^{\mathrm{SI}} \sqrt{E_s} a_{p,k}^{(q,p-q)} \times s_j(t)^q s_j^*(t)^{(p-q)} + n_i^R(t) \\ & i = 1, 2, \cdots, n_R, j = 1, 2 \end{aligned} \quad (40)$$

where h_{ik}^{SI} is the elements of the actual SI channel matrix.

Considering the active RF analog cancellation at the receiver, the SI signal is subtracted from each of the received signal after suitable gains and phase adjustments. We assume the RF analog canceller is single-tap in this paper and is denoted as $\mathbf{H}^{RF}$, the cancellation matrix operated on the PA output signals. After analog RF cancellation, the received signal at the relay becomes

$$\begin{aligned} \mathbf{y}^{RSI}(t) &= \mathbf{y}(t) - \mathbf{H}^{RF}\sqrt{E_s}\mathbf{s}^{PA}(t) \\ &= \mathbf{H}_{MA}\mathbf{x}(t) + \sqrt{E_s}\mathbf{H}^{RSI}\mathbf{s}^{PA}(t) + \mathbf{n}_R(t) \end{aligned} \quad (41)$$

where $\mathbf{H}^{RSI} = \mathbf{H}^{SI} - \mathbf{H}^{RF}$ denotes the $n_R \times n_T$ residual self-interference (RSI) channel after RF analog cancellation. For simplicity, we assume that $\mathbf{H}^{SI}$ and $\mathbf{H}^{RF}$ can be estimated at the RF receiver front end with several methods [42] and $\mathbf{H}^{RSI}$ is a Gaussian matrix whose elements are zero mean and variance λ random variables. The variance λ reflects the quality of RF analog cancellation. The smaller λ represents a high quality of analog cancellation at the RF front end. Then, substituting Eqs. (39) and (40) into Eq.(41), the RSI signal at the i-th receiver is given as

$$\begin{aligned} y_i^{\mathrm{RSI}}(t) &= y_i(t) - \sum_{k=1}^{n_T} h_{ik}^{\mathrm{RF}} \sqrt{E_s} s_k^{\mathrm{PA}}(t) \\ &= h_{ij}^{\mathrm{MA}} x_j(t) + \sum_{\substack{l=1\\l\neq j}}^{2} h_{il}^{\mathrm{MA}} x_l(t) \\ &\quad + \sum_{k=1}^{n_T} \sum_{\substack{p=1\\p\,\mathrm{odd}}}^{P} \sum_{q=0}^{p} h_{ik}^{\mathrm{RSI}} \sqrt{E_s} a_{p,k}^{(q,p-q)} \times s_j(t)^q s_j^*(t)^{(p-q)} + n_i^R(t) \\ & i = 1, 2, \cdots, n_R, j = 1, 2 \end{aligned} \quad (42)$$

where $h_{ik}^{\mathrm{RSI}} = h_{ik}^{\mathrm{SI}} - h_{ik}^{\mathrm{RF}}$ is the element of the matrix $\mathbf{H}^{RSI}$ and $y_i^{\mathrm{RSI}}(t)$ denotes the RSI signal at the i-th receiver after RF analog cancellation.

6.2 The Dempster-Shafer physical-layer network coding scheme under the self-interference signal model with nonlinear distortion

In this paper, since the best performance is obtained by the proposed DS-PNC scheme, the DS-PNC scheme is studied to suppress the RSI after analog RF cancellation. Similar to the processing methods in Section 3.3, the output signal vector $\sqrt{E_s}\mathbf{s}^{PA}(t)$ of PA is regarded as $\mathbf{x}_L(t)$ in Eq. (41). The framework of discernment is still selected as modulation constellation set Ψ. For BPSK, there are also three FESs considered in BPA computation and the combined transmit vector $\mathbf{x}_s(t) = [x_1(t), x_2(t), \sqrt{E_s}\mathbf{s}^{PA}(t)]^T$ is also divided into two groups. One group $E = \{[-1, -1, \sqrt{E_s}\mathbf{s}^{PA}(t)]^T, [1, 1, \sqrt{E_s}\mathbf{s}^{PA}(t)]^T\}$ corresponds to $x_1 \oplus x_2 = 1$ and the other group $F = \{[-1, 1, \sqrt{E_s}\mathbf{s}^{PA}(t)]^T, [1, -1, \sqrt{E_s}\mathbf{s}^{PA}(t)]^T\}$ corresponds to $x_1 \oplus x_2 = -1$. The elements of vector $\mathbf{s}^{PA}(t)$ belong to the set $\Lambda = \{\sum_{\substack{p=1\\p\,\mathrm{odd}}}^{P} \sum_{q=0}^{p} a_{p,j}^{(q,p-q)} \times s_j(t)^q s_j^*(t)^{(p-q)}\}, s_j(t) \in \Psi$. Because the cardinality of set Λ is M, the vector $\mathbf{s}^{PA}(t)$ has M^{n_T} possible vectors. So, the size of each group is also decided by the modulation constellation order M and the number of relay transmit antennas n_T. For all single-point FES A_1, the conditional PDF of $y_i^{\mathrm{RSI}}(t)$ is denoted by

$$\begin{aligned} & f(y_i^{\mathrm{RSI}}(t) \mid x_1 \oplus x_2 = -1) \\ &= \frac{1}{\sqrt{2\pi\sigma^2}} \sum_{\mathbf{x}_s(t)\in E} \exp\left[\frac{\| y_i^{\mathrm{RSI}}(t) - (h_{i1}^{\mathrm{MA}}, h_{i2}^{\mathrm{MA}}, \mathbf{h}_i^{\mathrm{RSI}})\mathbf{x}_s(t) \|^2}{2\sigma^2}\right] \\ & f(y_i^{\mathrm{RSI}}(t) \mid x_1 \oplus x_2 = 1) \\ &= \frac{1}{\sqrt{2\pi\sigma^2}} \sum_{\mathbf{x}_s(t)\in F} \exp\left[\frac{\| y_i^{\mathrm{RSI}}(t) - (h_{i1}^{\mathrm{MA}}, h_{i2}^{\mathrm{MA}}, \mathbf{h}_i^{\mathrm{RSI}})\mathbf{x}_s(t) \|^2}{2\sigma^2}\right] \\ & i = 1, \cdots, n_R \end{aligned} \quad (43)$$

where the $\mathbf{h}_i^{RSI}$ is the i-th row of the RSI channel. The groups E and F contain M^{n_T+1} possible vectors.

For two-point FES A_2, the BPA can be computed by Eq. (20). For QPSK, the BPAs are computed similarly as Eqs. (21) and (22). After obtaining the BPAs of all the FESs, Dempster's combination rule and the MC rule are used to obtain the network-coded signal.

7 Simulation results and analysis

In this section, compared with traditional spatial-domain schemes, BER performances of the proposed schemes are evaluated in a two-way FD MIMO relay system. For comparison, DS-PNC regarded as detection algorithm is applied to further suppress the residual SI after traditional spatial-domain schemes such as the MMSE filter. Hence, the combination of DS-PNC and the MMSE filter called the DS-PNC-MMSE scheme is also presented in this paper. For simplicity, we assume $n_R = 2$ and $n_T = 1$ or $n_T = 2$ at the relay. Meanwhile, BPSK and QPSK modulations are considered at all the nodes. The transmit power at each antenna is normalized to one. The signal-to-interference ratio (SIR) and the signal-to-noise ratio (SNR) are defined respectively as the ratio of the received useful signal power to the SI power and the ratio of the received useful signal power to the noise power at each receive antenna. In order to achieve better performance for traditional spatial-domain suppression schemes, maximum likelihood (ML) detection is used at the relay after spatial-domain suppression schemes in our simulation.

7.1 Simulation and discussion for the relay equipped with one and two transmit antennas

Firstly, compared with traditional spatial-domain schemes, BER performances of the proposed schemes in the MA phase are illustrated in Fig. 3 for the relay equipped with one transmit antenna and BPSK modulation. As shown in the figure, the proposed schemes are better than the traditional spatial-domain suppression schemes. Considering SIR $=$ 3 dB at the relay , DS-NC without iteration has a worse BER performance compared with the ZF filter. However, DS-NC with one iteration outperforms DS-NC without iteration by about 8 dB at a BER of 10^{-2} with a little complexity increase. Meanwhile, DS-NC with one iteration also outperforms the ZF filter and MMSE filter, which proves that iteration can indeed improve the performance and the DS-NC scheme at least needs one iteration to obtain better performance. In addition, compared with DS-NC, the proposed DS-PNC not only obtains about a 4-dB performance gain at a BER of 10^{-3} but also has a reduced complexity. Meanwhile, DS-PNC achieves the same diversity gain as ideal cancellation. The combined DS-PNC-MMSE has an inferior performance to DS-PNC and DS-NC with one iteration, but it outperforms the traditional spatial-domain schemes.

Considering $SIR = 0$ dB at each source node , the BER performance of the DS scheme at the source nodes is depicted in Fig. 4 for the BPSK modulation. Compared with the ZF and MMSE schemes, the DS scheme obtains obvious performance gain and achieves the same diversity gain as ideal cancellation.

In Fig. 5, end-to-end average BER performances of the proposed schemes are compared with traditional spatial-domain suppression schemes. As we all know, end-to-end average BER performance is decided by the worst link in two-way relay. From Figs. 3 and 4, we can see that the performances of the BC phase are better than those of the MA phase. So, end-to-end performances of all the schemes are similar to the performances in the MA phase.

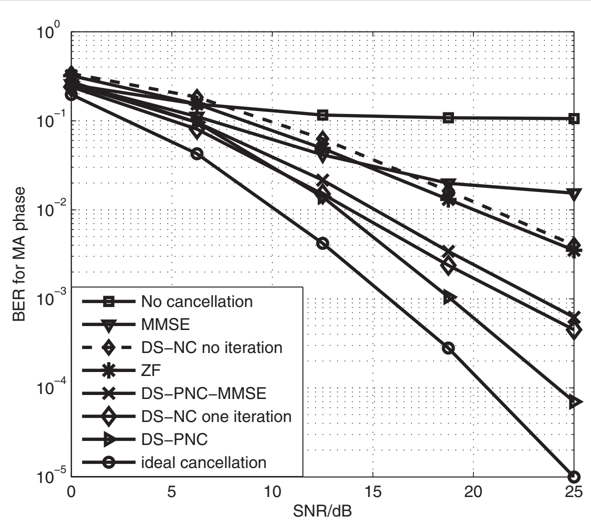

Fig. 3 BER performances for the relay equipped with one transmit antenna and BPSK modulation in the MA phase when SIR is 3 dB

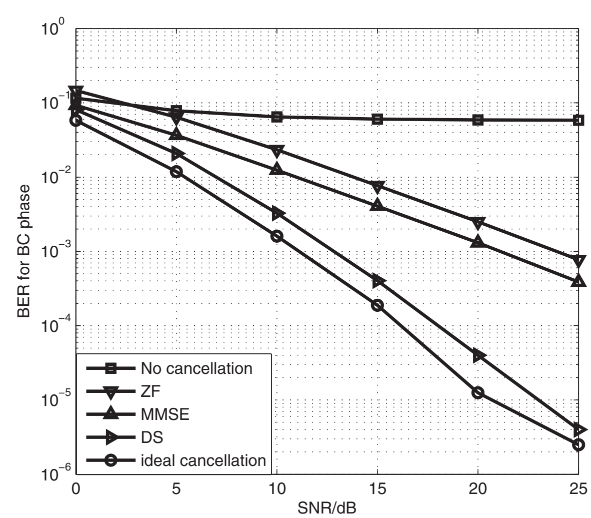

Fig. 4 BER performances for the relay equipped with one transmit antenna and each source node equipped with two receive antennas for BPSK modulation in the BC phase

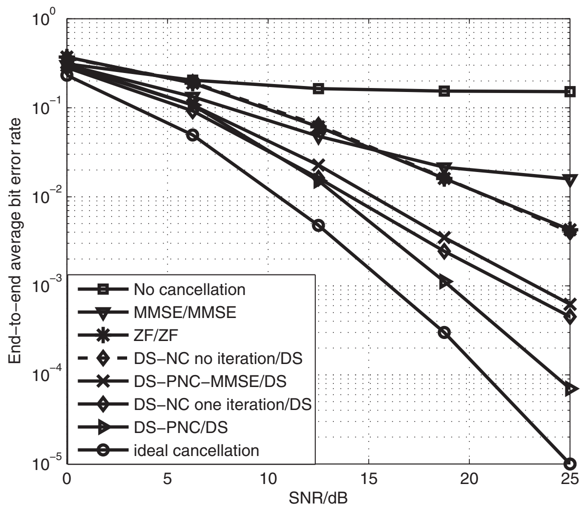

Fig. 5 End-to-end average BER performances for the relay equipped with one transmit antenna and BPSK modulation

As shown in Fig. 5, all the proposed schemes are better than the traditional schemes. The proposed DS-NC with one iteration/DS (the suppression scheme used at the relay/the suppression scheme used at the source nodes) obtains about a 5-dB performance gain at a BER of 10^{-2} compared with the traditional spatial-domain schemes. Furthermore, the proposed DS-PNC/DS is superior to DS-NC with one iteration/DS and has about a 6-dB gain than the traditional spatial-domain schemes at a BER of 10^{-2}. Similar to Fig. 3, the DS-PNC-MMSE/DS scheme is inferior to DS-PNC/DS and DS-NC with one iteration/DS but is superior to spatial-domain schemes.

Figure 6 depicts the BER performances in the MA phase for the relay with one transmit antenna and QPSK modulation. Similar to Fig. 3, the performances of all the proposed schemes are better than those of traditional schemes. For QPSK, the performance of DS-PNC-MMSE is similar to that of DS-NC with one iteration, which outperforms the traditional schemes by about 3 dB at a BER of 10^{-2}. Moreover, DS-PNC obtains about 2-dB gains over DS-NC with one iteration at a BER of 10^{-2} and has a lower complexity. Meanwhile, DS-PNC achieves the same diversity gain as ideal cancellation.

Figures 7 and 8 show the BER performances of the BC phase and end-to-end transmission for the QPSK modulation, respectively. Compared with traditional spatial-domain schemes, the proposed DS scheme in the BC phase obtains at least 7-dB gains at a BER of 10^{-3}. In addition, end-to-end average BER performance is still decided by the worst link between the MA and BC phases. Compared with Fig. 6, similar conclusions are obtained. The end-to-end average BER performances of the proposed schemes are much better than those of spatial-domain schemes. The proposed DS-NC with one iteration/DS is superior to spatial-domain schemes but is inferior to the DS-PNC/DS scheme. Moreover, the proposed DS-PNC/DS achieves the same diversity gain as ideal cancellation.

Secondly, considering the relay equipped with two transmit antennas, the BER performances of the DS scheme and traditional spatial-domain schemes are also discussed for the BPSK and QPSK modulations. In this situation, the relay selects one antenna to transmit the signal according to the antenna selection method mentioned in Section 4.

Figure 9 depicts the BER performances of different suppression schemes at the source nodes for QPSK in the BC

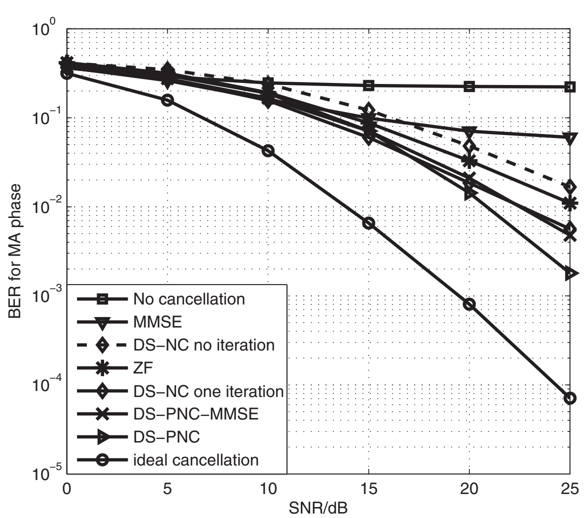

Fig. 6 BER performances for the relay equipped with one transmit antenna and QPSK modulation in the MA phase when SIR is 3 dB

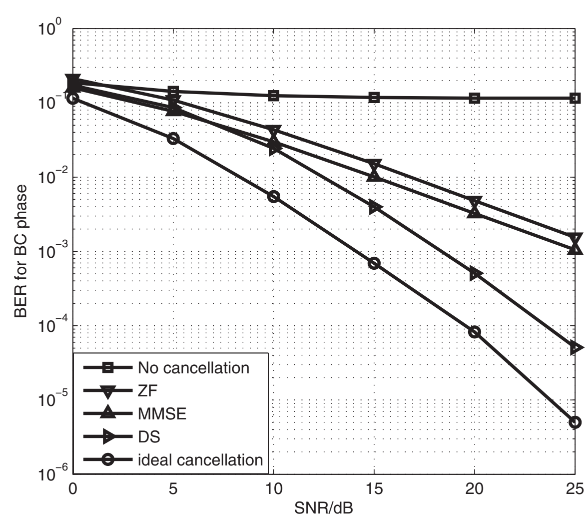

Fig. 7 BER performances for the relay equipped with one transmit antenna and each source node equipped with two receive antennas for QPSK modulation in the BC phase

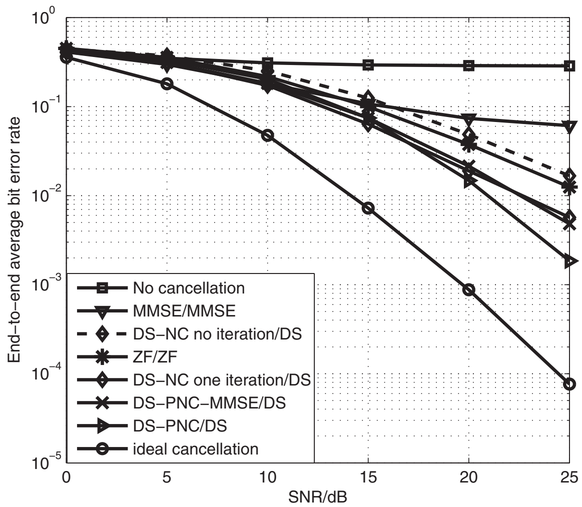

Fig. 8 End-to-end average BER performances for the relay equipped with one transmit antenna and QPSK modulation

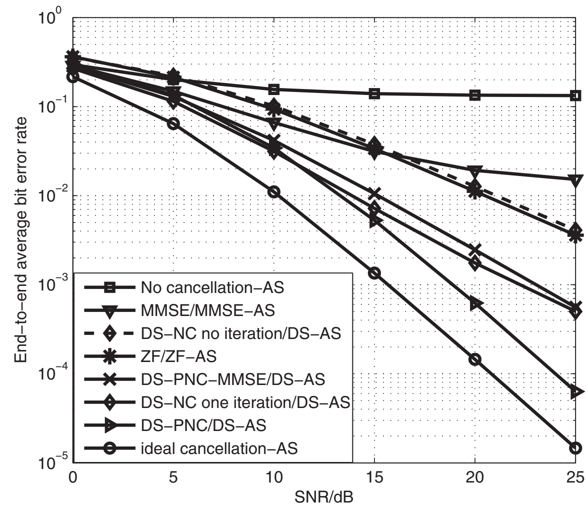

Fig. 10 End-to-end average BER performances for the relay equipped with two transmit antennas and the BPSK modulation. Antenna selection is used in the BC phase

phase. As shown in the figure, the similar results can be revealed that the DS scheme still obtains better performance than the traditional spatial-domain schemes. For comparison, we also present the performances of the relay with one transmit antenna. From the figure, we can see that for the same suppression scheme at the source nodes, the antenna selection scheme exploited at the relay with two transmit antennas has better BER performance than the relay equipped with one transmit antenna.

The end-to-end average BER performances of the proposed schemes are compared with the spatial-domain schemes in Fig. 10 for the relay with antenna selection and the BPSK modulation. Compared with Fig. 5, similar conclusions are obtained. The BER performances of the proposed schemes are much better than those of spatial-domain schemes. The proposed DS-NC with one iteration/DS-AS is superior to DS-PNC-MMSE/DS-AS and the spatial-domain schemes but inferior to the proposed DS-PNC/DS-AS. Moreover, the DS-PNC/DS-AS achieves the same diversity gain as ideal cancellation. Meanwhile, compared with Fig. 8, the similar results can be found in Fig. 11 for the QPSK modulation.

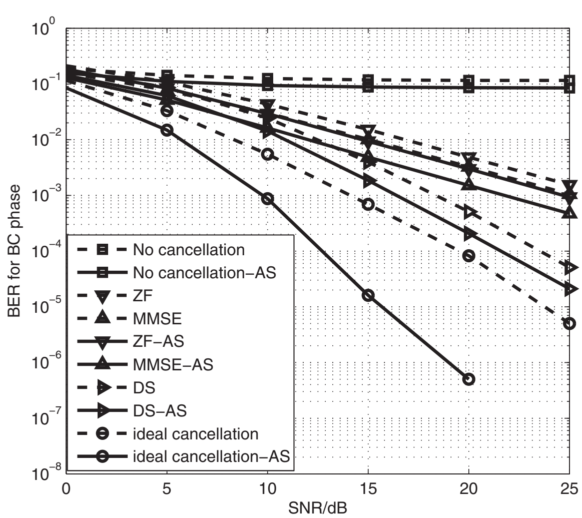

Fig. 9 BER performances for the relay with two transmit antennas and QPSK modulation in the BC phase. Antenna selection is used at the relay

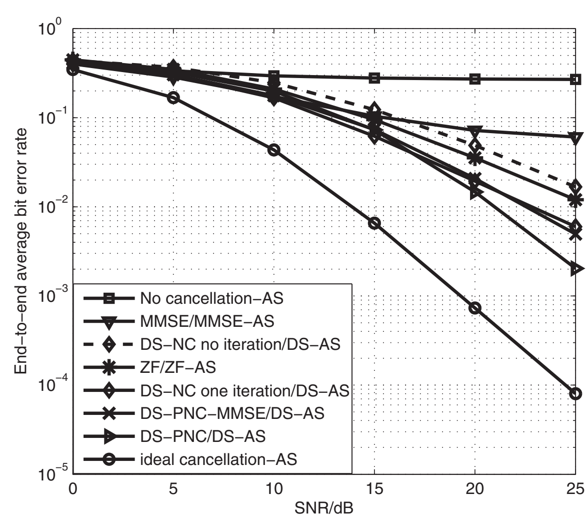

Fig. 11 End-to-end average BER performances for the relay equipped with two transmit antennas and the QPSK modulation. Antenna selection is used in the BC phase

7.2 Simulation results for the effects of different signal-to-interference ratio and channel estimation errors

In order to investigate the influence of different SIRs on the proposed schemes, Fig. 12 shows the BER performances of the proposed schemes and the MMSE filter suppression scheme in the MA phase when SNR is 25 and 30 dB, respectively, for the BPSK modulation. It can be showed that the BER performance of the MMSE filter scheme is improved obviously with SIR increased, but BER performances of the proposed DS-NC with one iteration and the DS-PNC schemes almost keep unchanged when SIR is varying. It means that the proposed schemes are more robust to SI than traditional spatial-domain schemes.

Considering channel estimation errors in both the MA and self-feedback channels, the BER performances of DS-PNC and the spatial-domain schemes are illustrated in Fig. 13 when SNR $=$ 20 dB and SIR $=$ 3 dB at the relay. As shown in the figure, the BER performances of DS-PNC and the spatial-domain schemes become worse when the variance of the channel estimation errors increased. Although the proposed DS-PNC scheme is a little more sensitive to the channel estimation errors than the traditional spatial-domain schemes. However, as mentioned above ,with the perfect channel state information, the proposed DS schemes outperform the spatial-domain schemes. Meanwhile, the proposed schemes are more robust to the SI and the DS-PNC scheme achieves the same diversity gain as the ideal cancellation. So, the proposed DS schemes are more suitable for the situation that has accurate channel estimation.

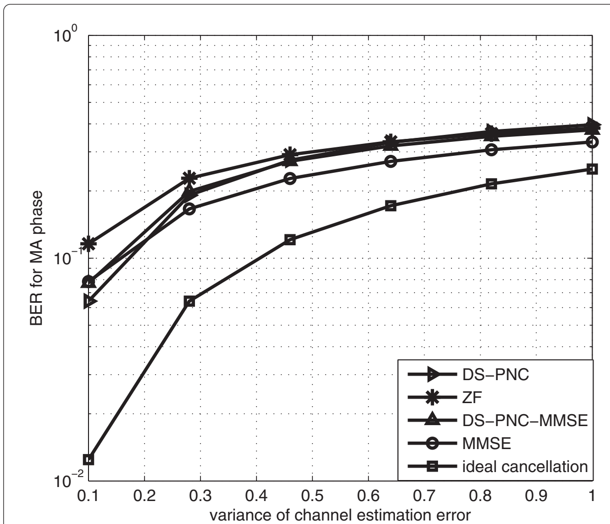

Fig. 13 The effect of channel estimation errors in the MA phase. The SNR of the MA phase is 20 dB, and the SIR at the relay is 3 dB

7.3 Simulation results under the self-interference signal model with nonlinear distortion

For simplicity, we assume that the PA nonlinear order P is three and the Taylor coefficients $a_{p,j}$ are set according to the reference [43]. The amplitude gains and phase parameters for I/Q imbalance are set as $\rho = 0.95$ and $\varphi = 5^{\circ}$ [44]. In Fig. 14, the BER performance of the proposed DS-PNC scheme with nonlinear distortion and RF analog cancellation is compared with spatial-domain suppression schemes in the MA phase. Considering $\lambda = 0.5$ after RF analog cancellation, it can be seen that the proposed DS-PNC scheme outperforms the ZF and MMSE filters by about 7 and 3 dB, respectively, at a BER of 10^{-2},

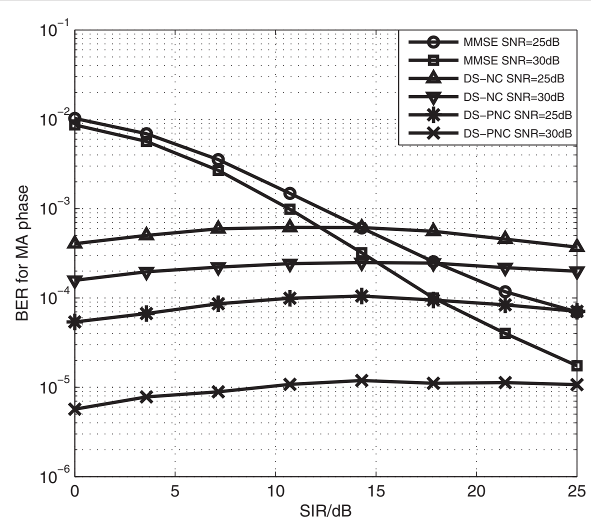

Fig. 12 BER performance comparison of different schemes in the MA phase for different SIR

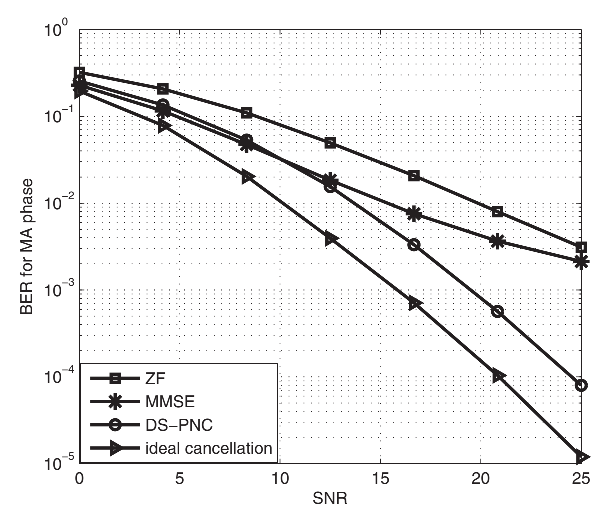

Fig. 14 BER performances with the relay equipped with one transmit antenna for the BPSK modulation in the MA phase when $\lambda = 0.5$

which proves that the DS-PNC scheme is also superior to the traditional schemes for considering the transmitter nonlinear distortion and RF analog cancellation. Meanwhile, DS-PNC also achieves the same diversity gains as ideal cancellation.

In order to investigate the effects of different RF analog cancellation quality on the proposed DS-PNC and traditional schemes, Fig. 15 depicts BER performances of the DS-PNC and traditional schemes with the coefficient λ varying in the interval $[0.1, 1]$ when the SNR is 20 dB. As shown in the figure, the BER performance of the MMSE filter becomes worse obviously with λ increasing but the performance of DS-PNC similar to that of the ZF filter almost keeps unchanged. It proves that the proposed DS-PNC scheme is more robust to the SI than the MMSE filter scheme no matter how the RF analog cancellation quality is. This conclusion is consistent with the results obtained in Fig. 12.

8 Complexity analysis

For the proposed schemes based on the DS theory, the complexities of the proposed schemes mainly depend on the complexities of the computations and combinations for multiple BPAs. There are $\frac{M^2+M}{2}$ uncertain decision propositions with only single-point and two-point FES considered in this paper, where M denotes the modulation constellation set cardinality. In [36], a BPA calculation or a combination of two BPAs is defined as a BPA evaluation. For simplicity, the complexities of the proposed schemes are determined by the number of BPA evaluation involved. According to [36], the complexity of a BPA evaluation is considered as $O(M^2)$ without existing SI. Considering the SI suppression in BPA computation, a BPA evaluation defined in this paper is the sum of M^{n_T} terms of the BPA computation. Therefore, the complexity of a BPA evaluation in this paper is approximately denoted by $O(M^{n_T+2})$.

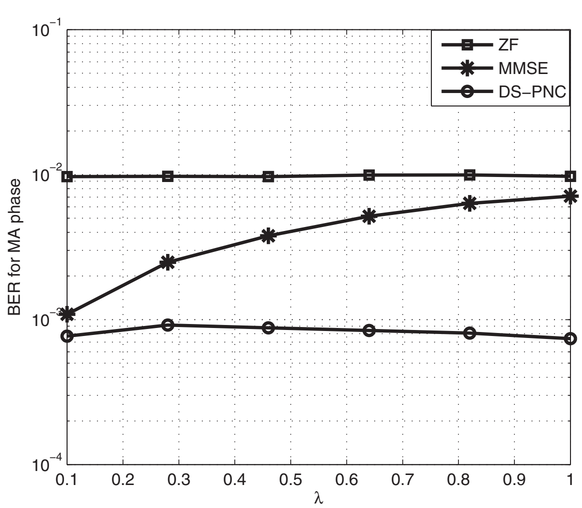

Fig. 15 BER performance comparison of different schemes in the MA phase with λ varying

For DS-NC without the iteration scheme, the complexity is mainly decided by the complexity of DS detection. The relay obtains n_{st} estimation signals for each receive antenna, where n_{st} denotes the number of all transmit antennas at the source nodes. Therefore, each receive antenna has n_{st} BPA evaluations. Since Dempster's combination rule is exploited to combine the BPAs from each receive antenna, the number of BPA evaluation can be expressed as $n_R n_{st}$. Therefore, the complexity of DS-NC without iteration is approximately $O(M^{n_T+2} n_R n_{st})$. With one iteration exploited in DS-NC, the complexity is increased to $O(2M^{n_T+2} n_R n_{st})$. However, the relay only has n_R BPA evaluations in DS-PNC because the signal detection is not needed at each receive antenna. So, the complexity is reduced to $O(M^{n_T+2} n_R)$. For comparison, the complexity of the MMSE SI suppression can be considered as $O(n_R{}^3)$ according to [45]. From the above analysis, the complexity of the proposed DS-PNC is lower than that of the proposed DS-NC.

9 Conclusions

In this paper, the novel SI suppression schemes based on the DS theory were proposed at the relay and source nodes for the two-way FD MIMO relay system. In the MA phase, DS-NC adopted the DS evidence theory to estimate the signals of each source node with SI considered in the BPA computation. Furthermore, the proposed DS-PNC scheme considered SI suppression from the vector space perspective and combined the PNC mapping rule with the DS theory to obtain the network-coded signal directly. For comparison, DS-PNC-MMSE that combined the DS-PNC and MMSE filter schemes was presented. In the BC phase, antenna selection was adopted at the relay and the DS scheme exploited at the source nodes was similar to DS-PNC but without considering the PNC mapping rule in the BPA computation. Meanwhile, the effects of imperfect SI channel estimation and the intended channel estimation on the proposed schemes was also studied. Finally, the proposed DS-PNC scheme was studied under the SI signal model with nonlinear distortion and RF analog cancellation. Simulation results revealed that the proposed DS-PNC scheme was a little more sensitive to the channel estimation errors than the traditional spatial-domain schemes. However, the proposed schemes outperformed spatial-domain schemes with the perfect channel state information. Furthermore, considering the SI signal model with nonlinear distortion and RF cancellation, the DS-PNC scheme was also superior to the traditional schemes and more robust to the SI. Meanwhile, the DS-PNC scheme achieved the same diversity gain as the ideal cancellation.

Competing interests
The authors declare that they have no competing interests.

Acknowledgements
This work is jointly supported by the National Natural Science Foundation of China under Grant 61201198, Beijing Natural Science Foundation of China under Grant 4132015, 4132007, and 4132019.

Received: 9 October 2015 Accepted: 3 April 2016
Published online: 18 April 2016

References

1. B Rankov, A Wittneben, Spectral efficient protocols for half-duplex fading relay channels. IEEE J. Sel. Areas Commun. **25**(2), 379–389 (2007)
2. C Eşli, A Wittneben, in *IEEE Global Telecommunications Conference*. One- and two-way decode-and-forward relaying for wireless multiuser MIMO networks (IEEE, New Orleans, USA, 2008), pp. 1–6
3. T Unger, A Klein, in *Proceeding of the 16th Imaging Systems and Techniques on Mobile and Wireless Communications Summit*. On the performance of two-way relaying with multiple-antenna relay stations (IEEE, Budapest, Hungary, 2007), pp. 1–5
4. I Hammerström, M Kuhn, C Eşli, J Zhao, A Wittneben, G Bauch, in *Proceeding of the 8th Workshop On Signal Processing Advances in Wireless Communications*. MIMO two-way relaying with transmit CSI at the relay (IEEE, Helsinki, Finland, 2007), pp. 1–5
5. M Peng, H Liu, W Wang, H-H Chen, Cooperative network coding with MIMO transmission in wireless decode-and-forward relay networks. IEEE Trans. Veh. Technol. **59**(7), 3577–3588 (2010)
6. CH Liu, F Xue, in *Proceeding of IEEE International Conference on Communications*. Network coding for two-way relaying: rate region, sum rate and opportunistic scheduling (IEEE, Beijing, China, 2008), pp. 1044–1049
7. S-YR Li, RW Yeung, N Cai, Linear network coding. IEEE Trans. Inf. Theory. **49**(2), 371–381 (2003)
8. Z Shengli, S-C Liew, PP Lam, Physical layer network coding. arXiv preprint arXiv: 0704.2475 (2007)
9. S Zhang, QF Zhou, C Kai, W Zhang, Full diversity physical-layer network coding in two-way relay channels with multiple antennas. IEEE Trans. Wirel. Commun. **13**(8), 4273–4282 (2014)
10. O Taghizadeh, R Mathar, in *Proceeding of the 18th International ITG Workshop On Smart Antennas*. Full-duplex decode-and-forward relaying with limited self-interference cancellation (VDE, Erlangen, Germany, 2014), pp. 1–7
11. AC Cirik, R Wang, Y Rong, Y Hua, in *Proceeding of the 15th International Workshop On Signal Processing Advances in Wireless Communications*. MSE based transceiver designs for bi-directional full-duplex MIMO systems (IEEE, Toronto, Canada, 2014), pp. 384–388
12. K Haneda, E Kahra, S Wyne, C Icheln, P Vainikainen, in *Proceeding of the 4th European Conference On Antennas and Propagation*. Measurement of loop-back interference channels for outdoor-to-indoor full-duplex radio relays (IEEE, Barcelona, Spain, 2010), pp. 1–5
13. W Slingsby, J McGeehan, in *Proceeding of the 9th International Conference on Antennas and Propagation*. Antenna isolation measurements for on-frequency radio repeaters (IET, Eindhoven, Holland, 1995), pp. 239–243
14. CR Anderson, S Krishnamoorthy, CG Ranson, TJ Lemon, WG Newhall, T Kummetz, JH Reed, in *Proc. IEEE SoutheastCon*. Antenna isolation, wideband multipath propagation measurements, and interference mitigation for on-frequency repeaters (IEEE, Greensboro, USA, 2004), pp. 110–114
15. H Hamazumi, K Imamura, N Iai, K Shibuya, M Sasaki, in *Proceeding of Global Telecommunications Conference*. A study of a loop interference canceller for the relay stations in an SFN for digital terrestrial broadcasting (IEEE, San Francisco, USA, 2000), pp. 167–171
16. KM Nasr, JP Cosmas, M Bard, J Gledhill, Performance of an echo canceller and channel estimation for on-channel repeaters in DVB-T/H networks. IEEE Trans. Broadcast. **53**(3), 609–618 (2007)
17. T Riihonen, S Werner, R Wichman, in *Proceeding of IEEE Conference Record of the Forty-Third Asilomar Conference On Signals, Systems and Computers*. Spatial loop interference suppression in full-duplex MIMO relays (IEEE, Pacific Grove, USA, 2009), pp. 1508–1512
18. B Chun, E-R Jeong, J Joung, Y Oh, YH Lee, in *Proceeding of 2009 Annual Summit and Conference*. Asia-Pacific Signal and Information Processing Association, Pre-nulling for self-interference suppression in full-duplex relays (IEEE, Sapporo, Japan, 2009), pp. 91–97
19. M Ahmed, CC Tsimenidis, SY Le Goff, in *Proceeding of the 10th International Conference On Wireless and Mobile Computing, Networking and Communications*. Performance analysis of full-duplex MIMO-SVD-SIC based relay in the presence of channel estimation errors (IEEE, Larnaca, Republic of Cyprus, 2014), pp. 467–472
20. T Riihonen, S Werner, R Wichman, Mitigation of loopback self-interference in full-duplex MIMO relays. IEEE Trans. Signal Process. **59**(12), 5983–5993 (2011)
21. Y Sung, J Ahn, B Van Nguyen, K Kim, in *Proceeding of IEEE International Symposium on Intelligent Signal Processing and Communications Systems*. Loop-interference suppression strategies using antenna selection in full-duplex MIMO relays (IEEE, Chiang Mai, Thailand, 2011), pp. 1–4
22. K Yang, H Cui, L Song, Y Li, in *Proceeding of IEEE International Conference On Communications*. Joint relay and antenna selection for full-duplex AF relay networks (IEEE, Sydney, Australia, 2014), pp. 4454–4459
23. P Lioliou, M Viberg, M Coldrey, F Athley, in *Proceeding of IEEE Record of the Forty Fourth Asilomar Conference On Signals, Systems and Computers*. Self-interference suppression in full-duplex MIMO relays (IEEE, Pacific Grove, USA, 2010), pp. 658–662
24. T Riihonen, A Balakrishnan, K Haneda, S Wyne, S Werner, R Wichman, in *Proceeding of the 45th Annual Conference On Information Sciences and Systems*. Optimal eigenbeamforming for suppressing self-interference in full-duplex MIMO relays (IEEE, Baltimore, USA, 2011), pp. 1–6
25. CYA Shang, PJ Smith, GK Woodward, H Suraweera, in *Proceeding of Australian Communications Theory Workshop*. Linear transceivers for full duplex MIMO relays (IEEE, Sydney, Australia, 2014), pp. 11–16
26. X Cheng, B Yu, X Cheng, L Yang, in *Proceeding of IEEE Military Communications Conference*. Two-way full-duplex amplify-and-forward relaying (IEEE, San Deigo, USA, 2013), pp. 1–6
27. G Bi, H Gao, T Lv, W Wang, in *Proceeding of IEEE Military Communications Conference*. Alamouti-based schemes for full-duplex two-way relay networks (IEEE, Baltimore, Maryland, 2014), pp. 1601–1607
28. J Yang, X Liu, Q Yang, in *Proceeding of the 14th International Symposium On Communications and Information Technologies*. Power allocation of two-way full-duplex AF relay under residual self-interference (IEEE, Incheon, Republic of Korea, 2014), pp. 213–217
29. G Zheng, Joint beamforming optimization and power control for full-duplex MIMO two-way relay channel. IEEE Trans. Signal Process. **63**(3), 555–566 (2015)
30. D Zeng, J Xu, G Xu, Data fusion for traffic incident detector using DS evidence theory with probabilistic SVMS. J. Comput. **3**(10), 36–43 (2008)
31. T Denoeux, A neural network classifier based on Dempster-Shafer theory. IEEE Trans. Syst. Man Cybern. Syst. Hum. **30**(2), 131–150 (2000)
32. L Qin, Y Li, Z He, J Lin, Y Lu, in *Proceeding of the 8th International ICST Conference On Communications and Networking in China*. Cooperative signal processing scheme for multiple-cell based on evidence theory (IEEE, Beijing, China, 2013), pp. 643–647
33. M Eslamifar, WH Chin, C Yuen, YL Guan, Performance analysis of two-step bi-directional relaying with multiple antennas. IEEE Trans. Wirel. Commun. **11**(12), 4237–4242 (2012)
34. G Shafer, A mathematical theory of evidence. Princeton University Press Princeton. **1** (1976)
35. J Xia, T Lv, DST-based combining scheme outperforms maximal-ratio combining. Electron. Lett. **46**(7), 536–537 (2010)
36. J Xia, T Lv, Y Li, in *Proceeding of the 70th Vehicular Technology Conference Fall*. A novel MIMO detection scheme based on DS evidence theory (IEEE, Anchorage, USA, 2009), pp. 1–5
37. C Chiong, Y Rong, Y Xiang, Channel estimation for two-way MIMO relay systems in frequency-selective fading environments. IEEE Trans. Wirel. Commun. **14**(1), 399–409 (2015)
38. F Zhaoxi, S Jiong, S Hangguan, in *Proceeding of Cross Strait Quad-Regional Radio Science and Wireless Technology Conference*. Comparison of channel estimation schemes for MIMO two-way relaying systems (IEEE, Harbin, China, 2011), pp. 719–722
39. L Anttila, Digital front-end signal processing with widely-linear signal models in radio devices, Ph.D. dissertation, Tampere University of Technology (2011)

40. J Cha, J Yi, J Kim, B Kim, Optimum design of a predistortion RF power Amplifier for multicarrier WCDMA applications. IEEE Trans. Microw. Theory Tech. **52**(2), 655–663 (2004)
41. Y Yang, B Kim, A new linear amplifier using low-frequency second-order intermodulation component feed-forwarding. IEEE Microw. Guided Wave Lett. **9**(10), 419–421 (1999)
42. L Anttila, D Korpi, V Syrjala, M Valkama, in *Proceeding of 2013 Asilomar Conference on Signals, Systems and Computers*. Cancellation of power amplifier induced nonlinear self-interference in full-duplex transceivers (IEEE, Pacific Grove, USA, 2013), pp. 1193–1198
43. L Anttila, Research on nonlinear and mobile communication key technology of RF power amplifier, PH.D. dissertation, Zhejiang University (2005)
44. A Gokceoglu, S Dikmese, M Valkama, M Renfors, Energy detection under IQ imbalance with single- and multi-channel direct-conversion receiver: analysis and mitigation. IEEE J. Sel. Areas Commun. **32**(3), 411–424 (2014)
45. J Benesty, Y Huang, J Chen, A fast recursive algorithm for optimum sequential signal detection in a BLAST system. IEEE Trans. Signal Process. **51**(7), 1722–1730 (2003)